Propagation of Interfacial Waves in Microgravity

François Quirion*, Marie-Claude Asselin, and Guy G. Ross*
INRS-Énergie et Matériaux, 1650 Montée Ste-Julie, Varennes QC, Canada J3X 1S2

1 Introduction

It is quite difficult to imagine how the world, as we know it, would react to the disappearance of gravity but one thing is sure, the most spectacular events would arise from the redistribution of liquid in its environment. For example, water wets rock and gravity keeps it embedded into the ocean. In the absence of gravity, the ocean would climb up the cliffs and cover every surface that it can wet. Ships, which are often coated with water repellent, would be trapped inside gigantic air bubbles wandering within the liquid volume. These events are unlikely to occur on earth, but similar phenomena, based on the same physicochemical principles, do occur in a reduced gravity environment such as the one provided by the space shuttle.

It is now generally accepted that the investigation of interfacial properties is essential to the development of materials science either on earth or in the absence of gravity. As a result, the Microgravity Sciences and Application Bibliography[1] reports many more papers in the section covering Fluids, Interfaces, and Transport than in its section on Metals, Alloys, and Composites.

In 1992, Dr. Rath, editor of the book Microgravity Fluid Mechanics,[2] stressed the importance '... to get a wider basis and a precise comprehension of the different and interesting microgravity fluid mechanics phenomena.' The same year, an article in *Science* reported[3] that several committees of microgravity researchers have agreed that the field of microgravity materials science needs '... to turn away from the current thrust of experimentation in orbit – into materials and processes that could quickly be commercialized – and dive unashamedly into good, old-fashioned basic research.'

The propagation of a wave at the liquid–air or liquid–liquid interface is one of these old-fashioned topics that lacks information in the absence of gravity. It is relevant to the management of fluids[4,5] as well as for the preparation and processing[6] of metals, glasses, polymers and their alloys, composites, and foams which are processed through the liquid state.

Perturbing interfacial waves often occur during aircraft and shuttle experiments and they are also expected aboard the space station.[7] Let's just mention that they are a consequence of the residual accelerations, also known as g-jitter, arising from aerodynamic forces, routine crew activity, and equipment operation.

The perturbing and wetting forces both determine the configuration of liquids in partly filled containers and it becomes important to understand how they relate to each other in order to predict the behaviour of liquid samples subjected to g-jitter in microgravity.

To do so, the propagation of sinusoidal waves was investigated for liquid–air systems both on earth and during parabolic flights. Reduced gravity was also simulated using Plateau's neutral buoyancy technique.[8] The dispersion relation[9] was used to describe the movement of the liquids inside the container. A previous investigation[10] showed that wetting governs the configuration of liquids in low gravity and one of the objectives of this work is to evaluate its effect on the propagation of interfacial waves.

2 Theoretical Background

This section summarizes the theoretical background necessary to understand the phenomena described in this article.

2.1 Wetting

In the absence of gravity, the mass distribution of a liquid within a container will depend on its ability to wet the container.

* To whom correspondence should be addressed.

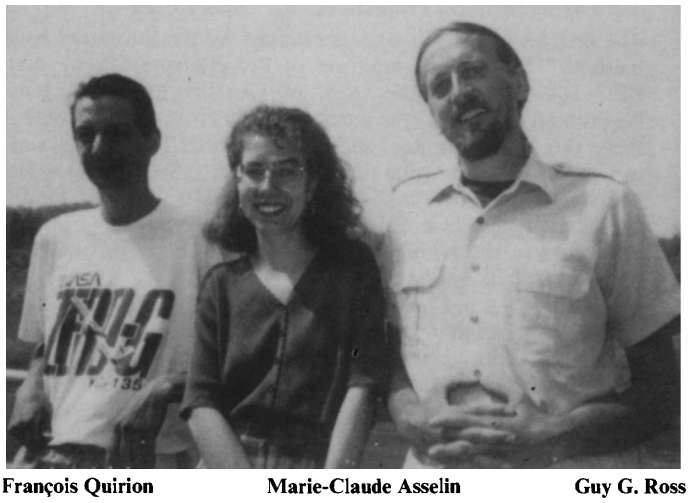

François Quirion Marie-Claude Asselin Guy G. Ross

François Quirion received his Ph.D. in Physical Chemistry at the Université de Sherbrooke in 1986. He also spent one year at the University of Tennessee, working on light and neutron scattering of micellar solutions. He is now professor at the INRS-Énergie et Matériaux. His research interests are related to the physical chemistry of interfaces, particularly interfacial tension and wetting phenomena applied to liquids in microgravity, polymer mixtures, and colloidal suspensions.

Marie-Claude Asselin is a third year Physics student at the Université de Sherbrooke. She participated in the ground and KC-135 experiments.

Guy G. Ross received his Ph.D. in Physics at the INRS-Énergie et Matériaux in 1985. He spent two years at the KFA-Juelich in Germany and three months at the Academia Sinica in China working on thermonuclear fusion. He is now professor at the INRS-Énergie et Matériaux. His research interests are related to the ion–matter interaction, ion beam modification of materials, and thermonuclear fusion.

Wetting is characterized by the contact angle, θ, that originates from the balance of the interfacial tension at the wall–liquid, $\sigma_{W/L}$, liquid–air, $\sigma_{L/A}$, and wall–air, $\sigma_{W/A}$, interfaces The correlation between the contact angle and the interfacial tensions is often referred to as the Young equation [11]

$$\cos(\theta) = (\sigma_{W\,A} - \sigma_{W\,L})/\sigma_{L\,A} \quad (1)$$

A well-known manifestation of wetting is the rise of a liquid on the surface of a material This forces the liquid interface to curve and the distance over which the curvature extends can be approximated by the capillary length, l_c In our case, the liquid is between two plates and

$$l_c = [\sigma\cos(\theta)/g\Delta\rho]^{\frac{1}{2}}, \quad (2)$$

where $\Delta\rho$ is the density difference between the fluid phases and g is the Earth gravitational acceleration For water in a plexiglass container with a contact angle of 55°, l_c is about 2 mm This implies that the curvature due to the capillary rise between the plates of the box, should not affect the interface at distances greater than about 2 mm from the walls However, a hundred-fold decrease of the gravitational acceleration will produce a tenfold increase of the capillary length to around 20 mm

2.2 Capillary Force

At low $g\Delta\rho$, the capillary length becomes large so that the radius of curvature of the meniscus, $t/2\cos(\theta)$, is constant over the thickness of the box, t For a box of length L, this creates a capillary force of magnitude

$$F_c = 2\sigma\cos(\theta)(L + t), \quad (3)$$

where $2(L + t)$ is the perimeter of the solid–liquid–air interface Hence, a perturbation will displace the liquid only if it generates a force, ma, greater than the capillary force In other words, a perturbation will change the configuration of the contained liquid only if it generates an acceleration,

$$a > 2\sigma\cos(\theta)(L + t)/m \quad (4)$$

where m is the mass of liquid

2.3 Interfacial Waves

The equation generally used to describe a sinusoidal wave at the interface of two fluids is the dispersion relation [9] Although this model does not account for the effect of wetting, it has been applied with success to the investigation of contained fluids

$$\omega_n^2 = k_n \frac{[g(\rho_1 - \rho_2) + \sigma k_n^2]}{[\rho_1 \mathrm{cotanh}(k_n h_1) + \rho_2 \mathrm{cotanh}(k_n h_2)]}, \quad (5)$$

where $k_n = 2\pi/\lambda_n$ and $\omega_n = 2\pi\vartheta_n$ with λ_n and ϑ_n being the wavelength and frequency of the resonance wave corresponding to mode n For a box of length L, λ_n is $2L/n$, and σ and ρ are respectively the interfacial tension and the density of the immiscible fluids in contact

For all the experiments described here, the containers were always filled with either coloured water and air or coloured water and a solution of heptane and carbon tetrachloride The interface was set at half height so that $h_1 = h_2 = h$ and thus equation 5 reduces to

$$\omega_n^2 = (g\,AG + \sigma k_n^2/(\rho_1 + \rho_2))k_n \tanh(k_n h), \quad (6)$$

where AG is the apparent gravity also referred to as the Atwood number,

$$AG = (\rho_1 - \rho_2)/(\rho_1 + \rho_2) \quad (7)$$

with subscript 1 standing for the lower and subscript 2 for the upper phase

Equation 6 contains a gravity and an interfacial tension contribution which will be referred to as the gravitational and interfacial waves, respectively At high frequencies the interfacial waves are independent of gravity, and their investigation – for instance by light scattering[12] – has proven an effective method for the determination of the interfacial tension of liquid–liquid and liquid–air systems

The investigation of low frequency interfacial waves is possible only when the apparent gravity or the gravity itself becomes small, for instance with immiscible liquids of similar density or during a curved trajectory where the centrifugal force balances gravity as in aircraft, rocket, and shuttle experiments

Figure 1 compares the patterns expected for the low frequency waves corresponding to mode 1 to 4 with those observed on earth for the gravitational waves in a half-filled container Notice that for all these modes, there is a node in the middle of the box The main difference between the real and expected patterns is due to the wetting of the liquid which causes distortion of the interface near the walls

The acceleration caused by a sine wave of amplitude A is $\pm A\omega^2$, and the variation of the amplitude of the wave at the interface, a, with the amplitude of the imposed sine wave, (da/dA), is defined here as the propagation efficiency At the resonance modes, a remains finite because of the viscosity of the liquid, η Kamotani and Ostrach[5] suggested a reciprocal square root dependence for the propagation efficiency with respect to the viscosity of Newtonian liquids

3 Experimental Part

3.1 Propagation of Perturbations

The container was a thin plexiglass box having a length of 95 mm and a height of 44 mm The liquid–air and liquid–liquid interfaces were positioned at half-height The width was 10 mm for the ground experiments and 15 mm for the parabolic flight experiments

The perturbation imposed was a sine wave fed to a x–y plotter on which the box was fixed It was parallel to the liquid–air or liquid–liquid interface with an amplitude between 2 and 60 mm

The resonance modes were identified at the frequency for which the amplitude of the extrema (see Figure 1) was maximum The amplitude of the wave at the interface, a, was determined for at least ten values of the amplitude of the imposed wave, A, and the relation was linear with a slope, (da/dA), corresponding to the propagation efficiency

3.2 Physicochemical Properties of the Liquids Used

The interfacial tension was determined by the Du Nouy ring method The aqueous mixtures of Polyethylene Glycol 400 PEG 400 used for the effect of viscosity all behaved as Newtonian liquids, *i e* the shear stress is a linear function of the shear rate in the range of shear rate studied The density was measured with a vibrating tube densimeter [13] The contact angle was determined by direct visualization of a drop of liquid standing on plexiglass Table 1 summarizes the physicochemical properties of the liquids used to calculate the resonance frequencies from equation 6

Heptane, C_7, and carbon tetrachloride, CCl_4, are completely miscible in each other but immiscible in water They were used to simulate a reduced gravity environment The density of the mixtures of C_7 and CCl_4 is compared with the density of water in Figure 2 The arrows indicate the systems that were investigated here The apparent gravity of these systems, see equation 7, is calculated from the density of the organic mixture and the density of water

When equilibrated with water, the mixtures of heptane and carbon tetrachloride wet the plexiglass walls with an angle smaller than 20° Thus, when water is on top, the system simulates wetting conditions, while it simulates non-wetting

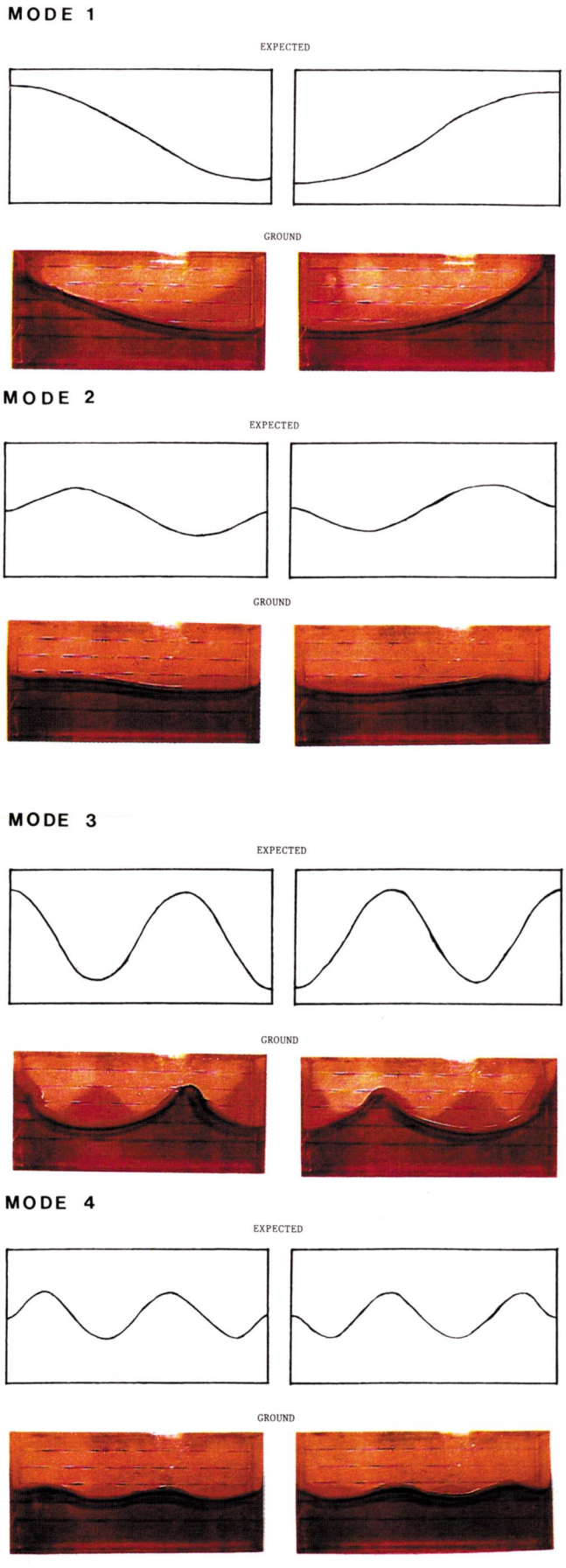

Figure 1 Comparison between the expected configuration of the liquid for mode one to four with the patterns observed at the liquid–air interface on the ground. The right and the left pictures represent the interface at time t and $t + 1/2\vartheta$, where ϑ is the frequency of the mode.

Table 1 Physicochemical properties of the liquids used in the course of the present investigations. All data for water imply the presence of a colorant.

	%	η (mPa.s)	ρ^a (kg/m^3)	σ (N/m)	θ (°)
Water	100	0.90	997	0.065	55
PEG 400	25.7	3.28	1044	0.040	49
	48.3	13.3	1085	0.033	31
	64.9	33.1	1105	0.041	38
C_7	100		679	0.018[b]	0[c]
CCl_4	100		1584	0.018[b]	0[c]

[a] Densities were obtained at 25 °C. [b] Interfacial tension between coloured water and mixtures of heptane and carbon tetrachloride. [c] The liquids spread on the plexiglass surface.

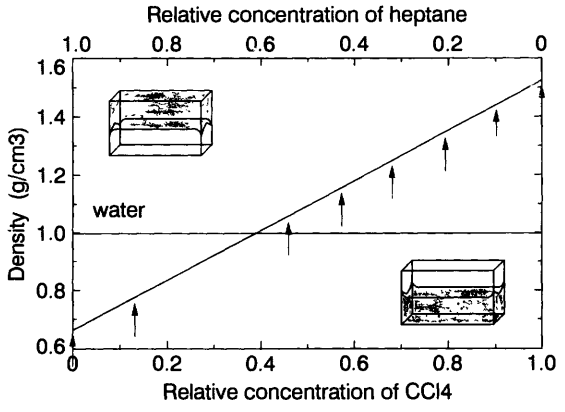

Figure 2 Density of the organic mixtures of heptane, C_7, and carbon tetrachloride, CCl_4. The horizontal line is the density of water in equilibrium with the organic mixtures and the arrows indicate the systems investigated during this work. The dotted line represents the isodensity condition where the organic phase (shaded) becomes heavier than water.

conditions when water sits at the bottom with respect to the earth acceleration (see Figure 2).

3.3 Parabolic Flight Experiments

It is important to realize that in aircraft and shuttle experiments, the gravitational force does act on the systems. For instance, an object orbiting at an altitude of 1600 km still senses 64% of the gravitational attraction of the Earth,[14] *i.e.* 0.64 *g*. This is much higher than the 0.001 *g* encountered aboard spaceships. The reduced gravity arises from a balance of the centrifugal and gravitational forces that act on the vehicles as they orbit around the earth.

The experiments presented here were performed aboard NASA's KC-135 aircraft, a modified Boeing 707, based in Houston, USA. During a typical parabola the aircraft undergoes about 25 seconds of reduced gravity. Because of pilot's manoeuvres and climatic disturbances, the level of gravity usually fluctuates in the range $\pm$ 0.01 *g*. The acceleration perpendicular to the liquid–air interface, z and parallel to the interface, y, are shown in Figure 3 along with a typical trajectory of the aircraft during a parabola.

In the absence of the imposed sine wave, the interface remained almost flat so that the residual accelerations originating from the aircraft could not be responsible for the large interfacial deformations associated to the resonance modes.

4 Results and Discussion

Three types of experiments were conducted during this investigation. Ground experiments with liquid–air systems where the

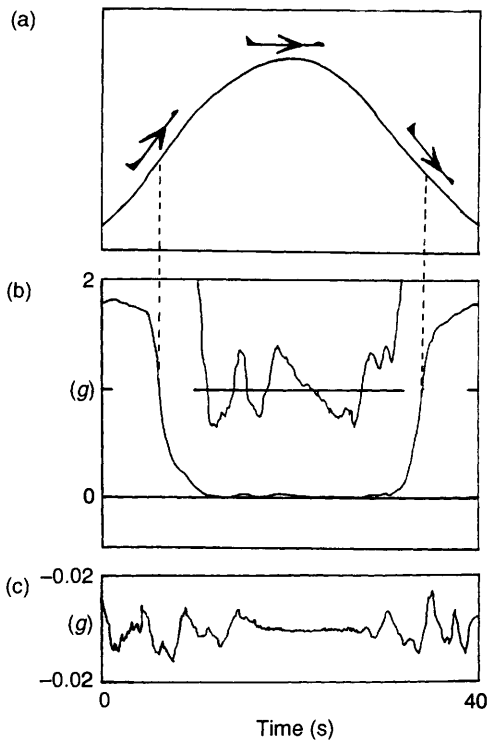

Figure 3 Accelerations obtained during a typical parabola at the centre of gravity of the aircraft: (a) trajectory of the aircraft; (b) acceleration level along the z-axis (top–bottom) including a magnification of the reduced gravity region; (c) acceleration along the y-axis (right–left).

capillary length, 2 mm, was always smaller than the thickness of the box, 10 mm. Ground simulations of reduced gravity with liquid–liquid systems where the capillary length was between 2 and 4 mm – still smaller than the thickness. Finally, parabolic flight experiments with liquid–air systems subjected to residual accelerations of about 0.01 g where the capillary length increases to about 20 mm while the thickness of the box was 15 mm.

4.1 Propagation at the Liquid–Air Interface on Earth

In these systems, the capillary length is smaller than the thickness so that wetting should not much affect the propagation of the waves. Figure 4 shows that the experimental resonance modes for water and aqueous solutions of PEG 400 in equilibrium with air compare very well with the frequencies calculated from equation 6. For a liquid–air interface on Earth, these resonances are mainly due to the gravity contribution and they are not expected to depend much on the surface properties. The results also show that the resonance modes do not depend on the viscosity, at least for the Newtonian liquids studied.

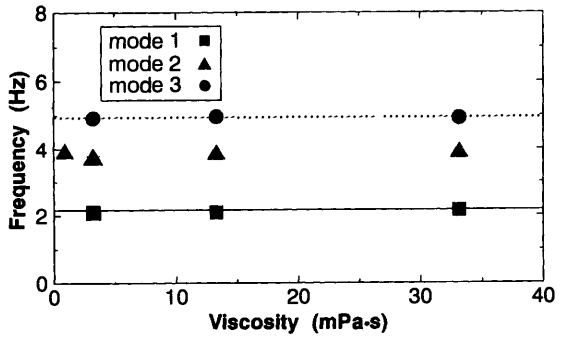

Figure 4 Experimental resonance frequency for modes 1, 2, and 3 at the air–liquid interface as a function of the viscosity of the liquid. Half-filled thin box (L = 0.095, H = 0.044, W = 0.010 m).

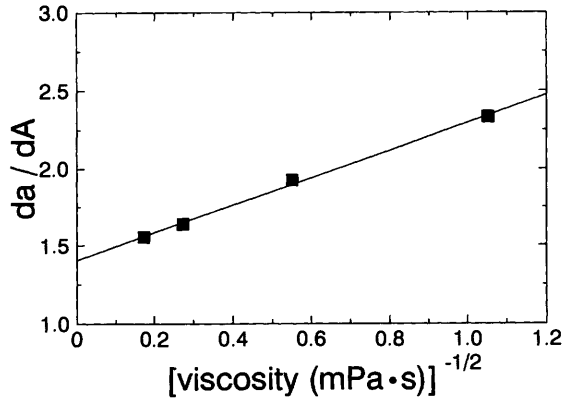

Figure 5 Reciprocal square root dependence of the propagation efficiency with the viscosity of the liquid for the propagation of mode 2 at the liquid–air interface. Half-filled thin box (L = 0.095, H = 0.044, W = 0.010 m).

The propagation efficiency was determined experimentally for mode 2 as a function of viscosity and the results are plotted in Figure 5. The reciprocal square root dependence reported by Kamotani and Ostrach[5] also applies to our data over the viscosity range investigated.

4.2 Reduced Gravity Simulation with Immiscible Liquid Mixtures

The dispersion relation also applies to liquid mixtures having different densities and it can be used to calculate their resonance modes. The major advantage of these systems is the possibility to reduce, at will, the gravity contribution to the resonance modes.

In such immiscible liquid mixtures, the gravitational force may be partially or totally balanced with the hydrostatic force. Mathematically, a decrease of g or AG, which is related to the density difference between the immiscible liquids, should affect the gravitational contribution in the same way (see equation 6).

As the apparent gravity decreases, the resonance modes become dominated by the interfacial tension contribution. This is shown in Figure 6 where a decrease of the gravitational contribution also results in a decrease of the frequency of the resonance modes. This explains the impression that liquids in space are in slow motion; they respond to lower frequencies. At the lower values of AG, the experimental frequencies seem systematically higher than the calculated ones. These systems correspond to capillary lengths around 6 mm so that wetting forces arising from the 10 mm thick boxes may begin to interfere with the dispersion of the waves.

As expected, the propagation efficiency decreases with the apparent gravity of the systems. A straightforward prediction is that the propagation of a mode will vanish when the density

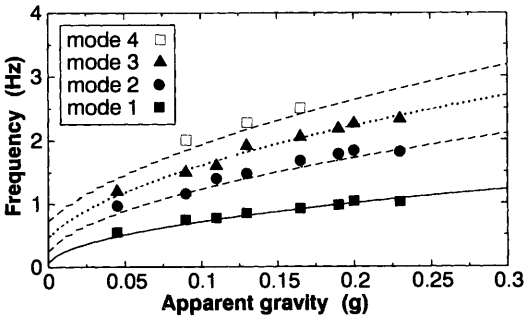

Figure 6 Experimental resonance frequency of modes 1 to 4 at the liquid–liquid interface with respect to the apparent gravity. Half-and-half mixtures of water and organic liquid consisting of heptane and carbon tetrachloride in a thin box (L = 0.095, H = 0.044, W = 0.010 m).

difference becomes zero. In such isopycnic (or isodensity) condition, there is no density gradient upon which the acceleration can act so that the system behaves as if its mass was homogeneously distributed inside the container. The propagation efficiency does in fact extrapolate to zero when the apparent gravity is zero as seen in Figure 7.

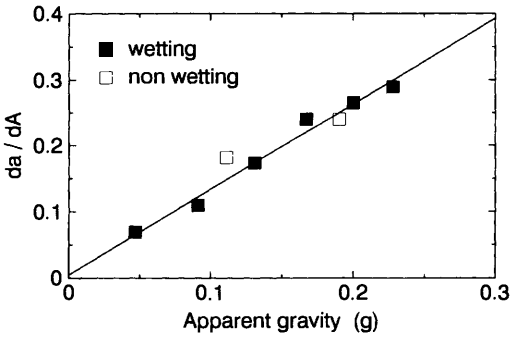

Figure 7 Linear dependence of the propagation efficiency of mode 2 at the liquid–liquid interface with respect to the apparent gravity. Half-and-half mixtures of water and organic liquid consisting of heptane and carbon tetrachloride in a thin box ($L = 0.095$, $H = 0.044$, $W = 0.010$ m).

At high C_7 content, the organic phase stands on top of the water phase so that the interface is curved downwards, as opposed to high CCl_4 content where the interface is curved upwards. Two systems with downward curvature were investigated and their frequencies and propagation efficiency are the same as their parent systems with upward curvature. In the systems studied, the gravitational contribution is still quite high (> 0.05 g) and it may overwhelm the wetting contribution arising from the thickness. Much lower levels, 0.01 g, are attained in the course of parabolic flights experiments, where the liquid–air interface may be investigated directly.

4.3 Perturbation in Microgravity

Parabolic flights experiments allowed us to investigate the propagation of interfacial waves at the liquid–air interface. However, the fluctuation in the level of acceleration during a parabola also causes the resonance frequency to oscillate around the constant frequency of the sine wave imposed on the system. Fortunately, the effect of the residual acceleration decreases rapidly for higher modes. For instance, at 0.01 g, the resonance frequency of the first mode may increase by 100% while it will cause only a 10% increase for the third mode.

The patterns of modes 2 and 4 as observed in reduced gravity are compared with their corresponding ground patterns in Figure 8. The first observation is the distortion of the interface which is affected by wetting forces. The extension of the curvature to larger distances is a consequence of the increase of the capillary length as discussed earlier.

The curvature also extends in the direction of the thickness of the boxes so that it generates a capillary force that stabilizes the interface. Figure 9 compares the response of four liquid samples to a given perturbation in the course of a parabola. The thickness of the boxes increases from 5 to 20 mm and they all contain a 50/50 mixture of coloured water and PEG 400. The curvature of the liquid–air interface in the thinner box, top left, extends to about 20 mm, in accordance with the increase of the capillary length due to the reduced gravity. The picture was taken just after a perturbation parallel to the interface and one can see that the liquid in the thinner box did not respond much while that in the thicker box, bottom right, did. This is in accordance with the occurrence of a stabilizing capillary force in thinner containers.

Once the liquid starts moving, it does so with either an advancing or a receding contact angle with the solid surface.

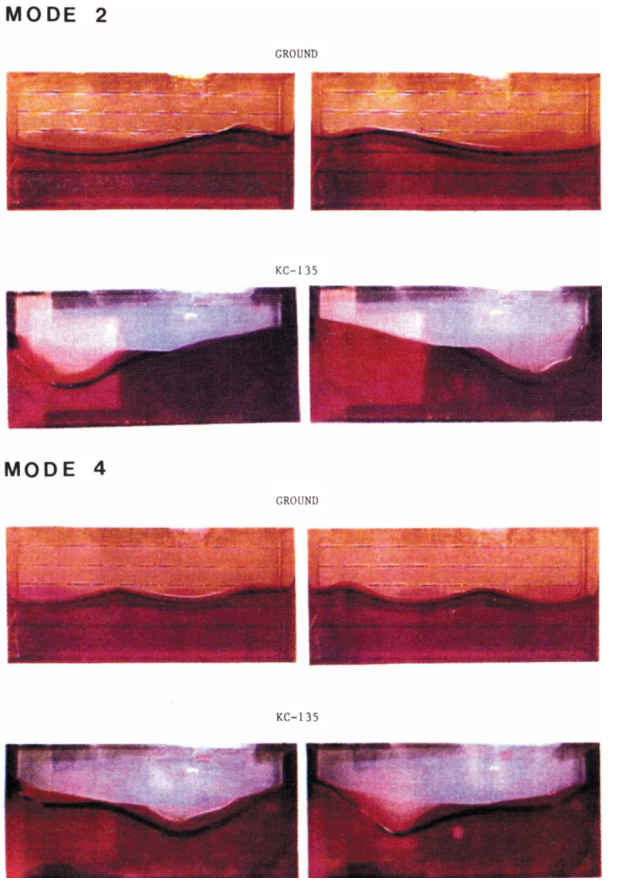

Figure 8 Comparison between the ground configuration of the liquid for mode two and four with the patterns observed in the course of KC-135 parabolic flight experiments. The right and the left pictures represent the interface at time t and $t + 1/2\vartheta$ where ϑ is the frequency of the mode. The box dimensions are $L = 0.095$, $H = 0.044$, $W = 0.015$ m.

Figure 9 This picture shows the effect of thickness on the response of the liquid–air interface to a perturbation. The thicknesses are 0.005, 0.010, 0.015, and 0.020 m for the top left, top right, bottom left, and bottom right boxes, respectively. The other dimensions of the boxes are $L = 0.22$ and $H = 0.12$ m.

These are different from each other, the advancing always being greater (or equal for ideal systems) than the receding, as illustrated in Figure 10. This is also true for the liquid that flows up and down in our flat boxes due to the imposed sine wave parallel to the interface. Hence, the change of contact angle, θ, upon rising or falling will affect the stabilizing capillary force (see equation 3).

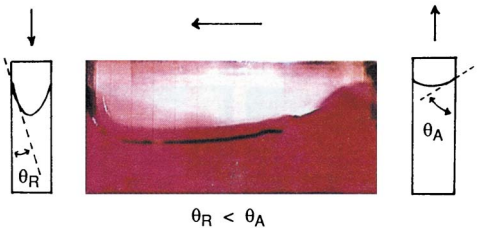

Figure 10 Picture of the liquid–air interface following a sudden right to left perturbation. The resulting advancing, θ_A, and receding, θ_R, contact angles of the liquid between the plates are also shown.

In our case, the liquid wets the wall and the curvature is downward with respect to gravity. Thus, the rise of the liquid occurs with an advancing contact angle while its fall occurs with a receding contact angle. According to equation 3 and knowing that the advancing contact angle is always greater than the receding, the stabilizing capillary force will be smaller when the liquid rises than when it falls. The consequence is that the liquid will rise on both sides of the box as shown in Figure 11. This results in a stable configuration where the interfaces are almost perpendicular to the imposed perturbation. This stresses the importance of the contact angle on the configuration of contained liquids and the propagation of perturbations within such systems.

Another phenomenon often observed in the course of a parabolic flight is the complete wetting of the container by the liquid which results in the encapsulation of air. For this to occur, the force caused by the acceleration due to the perturbation must be greater than the capillary force acting against the rise of the liquid on the side of the box. Figure 12 shows an encapsulation

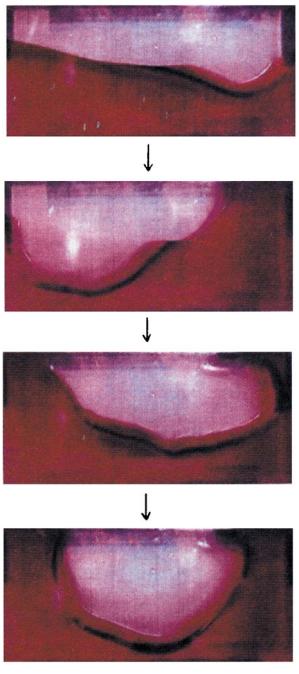

Figure 11 Sequence of events during a parabola which shows the rise of the liquid on both sides of the container leading to a U-shaped configuration. The box dimensions are $L = 0.095$, $H = 0.044$, $W = 0.015$ m.

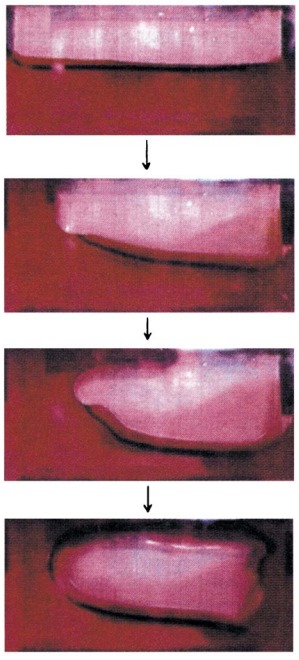

Figure 12 Sequence of events during a parabola which shows the encapsulation of air due to a y-perturbation. The box dimensions are $L = 0.095$, $H = 0.044$, $W = 0.015$ m.

as it progresses from a flat to a circular interface through the sloshing of the liquid on the side of box.

For our experiment, placed at the centre of gravity, the typical y-perturbations were too small to cause encapsulation ($\pm$ 0.005 g). However, when a sine wave parallel to the interface was imposed, encapsulation was observed for accelerations ($A\omega^2$) between 0.017 and 0.026 g. Assuming that these accelerations act on the total mass of liquid in the container, equation 4 leads to a contact angle for coloured water on plexiglass in the range 66° to 52°, respectively, in good accordance with the observed contact angle of 55° reported in Table 1.

The encapsulation of air into the liquid phase generates a circular interface that may resonate, or not, with the perturbation. The two situations are shown in Figure 13 where, at the lowest frequency, one can clearly observe a wave rolling around the bubble. This is not the case at the higher frequency where the bubble is broken into smaller bubbles that remain evenly distributed within the box.

5 Conclusions

It was shown that the dispersion relation applies to the propagation of perturbations at the liquid–air and liquid–liquid interface both on the ground and in the reduced gravity environment provided by parabolic flight experiments. The increase of the capillary length in microgravity enhances the wetting forces resulting in the deformation of the interface that may interfere with the usual propagation of a perturbation. For instance, it is suggested that the force generated by a perturbation must be greater than the stabilizing capillary force in order to displace the contained liquid. Under such conditions, the liquid may encapsulate the air and thus form a circular interface that may or may not resonate with the perturbation frequency.

Acknowledgments. The authors wish to thank M. Jacques Pelletier for technical support and they express their sincere gratitude to Lawrence Vézina, CSA, and Glenn Campbell, CSA, whose advice and help were greatly appreciated. The research described in this paper is part of a project financed by the Canadian Space Agency.

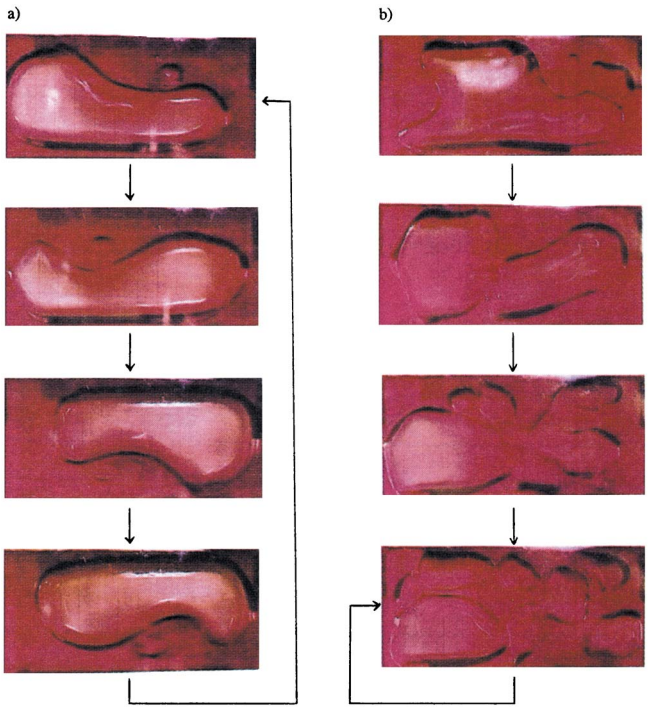

Figure 13 Comparison between a circular interface that (a) resonates with the imposed perturbation and (b) does not resonate with the imposed perturbation. The box dimensions are $L = 0.095$, $H = 0.044$, $W = 0.015$ m.

6 References

1 'Microgravity Science and Application Bibliography'. 1991 Revision, NASA Technical Memorandum #4348.

2 'Microgravity Fluid Mechanics', ed. H. J. Rath, Springer-Verlag, Berlin-Heidelberg, 1992.

3 Ivan Ammato, 'Microgravity Materials Science Strives to Stay in Orbit', *Science*, 1992, **257**, 882.

4 For instance see: R. J. Hung, C. C. Lee, F. W. Leslie, *Advances in Space Research*, 1991, **11**, 201—208 & 209—216; D. Langbein, *Microgravity Science and Technology*, 1992, **2**, 73—85; M. Weislogel, 'Forum on Microgravity Flows', American Society of Mechanical Engineers, New York, 1991, pp. 11—13.

5 Y. Kamotani and S. Ostrach, *J. Thermophysics and Heat Transfer*, 1989, **1**, 83.

6 For a review see: 'Fluid Sciences and Materials Science in Space', ed. H. U. Walter, Springer-Verlag, Berlin-Heidelberg, 1987.

7 E. S. Nelson, 'An Examination of Anticipated g-Jitter on Space Station and its Effects on Materials Processes', NASA Technical Memorandum #103775, April 1991.

8 J. A. F. Plateau, 'Statique expérimentale et théorique des liquides soumis aux seules forces moléculaires', Gauthier-Villars, Paris, 1873.

9 K. O. Mikaelian, *Phys. Rev.*, 1990, **A42**, 7211.

10 F. Quirion, in proceedings of Spacebound 92, Canadian Space Agency, Ottawa, 1992, pp. 83—87.

11 T. Young, *Philos. Trans. R. Soc. London*, 1805, **95**, 65. The topic of wetting has recently gained in popularity. For instance, see: 'Wettability', ed. John C. Berg, Marcel Dekker Inc., New York, Surfactant Science Series, Vol. 49, 1993; 'Contact Angle, Wettability, and Adhesion', ed. K. L. Mittal, VSP, Utrecht, 1993.

12 For an exhaustive review of these techniques see 'Light Scattering by Liquid Surfaces and Complementary Techniques', ed. D. Langevin, Marcel Dekker Inc., New York, Surfactant Science Series, Vol. 41, 1992.

13 P. Picker, E. Tremblay, and C. Jolicoeur, *J. Soln. Chem.*, 1974, **3**, 377.

14 These numbers were taken from a recent book, 'Fundamentals of Low Gravity Fluid Dynamics and Heat Transfer', ed. B. N. Antar and V. S. Nuotio-Antar, CRC Press, 1993.